

Requirements for Cosmological 21cm Masers

Mark Dijkstra^{1*} and Abraham Loeb^{2†}

¹*School of Physics, University of Melbourne, Parkville, Victoria, 3010, Australia*

²*Astronomy Department, Harvard University, 60 Garden Street, Cambridge, MA 02138, USA*

23 February 2019

ABSTRACT

We explore the prospects for a population inversion in the hyperfine levels of atomic hydrogen at high redshifts when the Universe was still predominantly neutral. The existence of 21-cm masers during the epoch of reionisation (EoR) could greatly boost the expected EoR signals. We perform Monte-Carlo calculations of the radiative transfer of Ly α photons emitted by a source embedded in a neutral collapsing gas cloud and compute the Ly α spectrum as function of radius and time. In such scenarios, the Ly α color temperature may be negative in large volumes surrounding the source. Classically, for sources with Ly α luminosities exceeding $\sim 10^{44} - 10^{45}$ erg s⁻¹, a population inversion in the hyperfine transition via the Wouthuysen-Field effect is established, thus resulting in a 21-cm maser. However, quantum interference can strongly reduce the strength of the WF-effect in the Ly α line wings, which implies that the required Ly α luminosities should be larger by orders of magnitude. Furthermore, we show that the astrophysical conditions that are required to establish a population inversion are very difficult to meet: A low flux of Ly α photons produced via x-ray and/or cosmic ray heating, or through cascades of atoms which are photo-excited by higher Lyman-series photons, can cause T_α to become positive. If, despite these obstacles, 21-cm masers do exist then we find that the background Cosmic Microwave background could be amplified by a maximum factor of ~ 100 , and maser saturation is not important.

Key words: cosmology: theory–radiative transfer–galaxies: high-redshift

1 INTRODUCTION

Detecting the redshifted HI 21-cm line from the epoch of reionisation is among the greatest observational challenges in present-day cosmology. Experiments such as the Low Frequency Array (LOFAR)¹, the Primeval Structure Telescope (PAST, Peterson et al. 2006) and the Mileura Widefield Array (MWA)², are currently being developed with the goal to detect this *Epoch of Reionisation* (EoR) signal within the next few years.

The strength and sign of the EoR signal depend on the spin temperature of the hydrogen gas, T_s , which is defined through the ratio of atoms in the ground and excited states of the hyperfine transition in the electronic ground state of hydrogen, $n_2/n_1 \equiv g_2/g_1 \exp[-T_*/T_s]$, where the ground and excited states are denoted by the labels '1' and '2', respectively and $T_* = 0.068$ K. If we denote the temperature of the Cosmic Microwave Background (CMB) by T_{CMB} , then neutral hydrogen gas can be seen in emission if $T_s > T_{\text{CMB}}$.

When $T_s < T_{\text{CMB}}$, the neutral hydrogen gas can be seen in absorption against the the CMB.

The distribution of atoms in the hyperfine levels is affected by collisions among the atoms as well as absorption and re-emission of the Cosmic Microwave Background (CMB) photons. Because of these interactions, the spin temperature is a weighted mean of T_{CMB} and T_{gas} (the gas temperature), where the weight of each is determined by the rates at which atoms collide and CMB photons are absorbed (Scott & Rees 1990; Loeb & Zaldarriaga 2004). At $z \gtrsim 200$ Thomson scattering by residual free electrons off the CMB keeps the gas, CMB and the spin temperatures nearly equal (Peebles 1993). Below this redshift, the gas adiabatically cools more rapidly than the CMB. At high enough redshifts, collisions are abundant and the spin temperature is locked to the gas temperature until at $z \lesssim 30$ the spin temperature rises back to the CMB temperature (see Fig.1 of Loeb & Zaldarriaga 2004).

The gas temperature and density increases in objects that collapse adiabatically, and the first gravitationally-bound *mini-halos* may be detectable in 21-cm emission (e.g. Iliev et al. 2002). The physics becomes more complex once the first sources form. The ionizing photons emitted by these sources photoionise the gas in their immediate

* E-mail: dijkstra@physics.unimelb.edu.au

† E-mail: aloeb@cfa.harvard.edu

¹ www.lofar.org

² <http://www.haystack.mit.edu/ast/arrays/mwa/site/index.html>

surroundings. Various processes, such as x-ray heating (Venkatesan et al. 2001; Pritchard & Furlanetto 2006b) and shock heating (Furlanetto & Loeb 2004) may heat neutral gas surrounding these HII bubbles to temperatures well above the CMB temperature (Furlanetto 2006). At this epoch, an additional process that may mix the populations in the hyperfine levels is through absorption and re-emission of Ly α photons, that were either emitted by nearby sources, produced as local recombination emission, or in cascades following photo-excitation by photons with energies $E \in [10.2 - 13.6]$ eV (Pritchard & Furlanetto 2006a). When the Ly α scattering rate dominates the collisional and CMB scattering rate, the hydrogen spin temperature, T_s , approaches the Ly α color temperature, T_α (Wouthuysen 1952). Field (1959) showed that resonant scattering of Ly α photons through an optically thick medium, redistributes the photons in frequency space according to a thermal distribution in a narrow region around the line center, making $T_\alpha = T_{\text{gas}}$. This is known as the 'Wouthuysen-Field' (hereafter WF) effect. Because of this effect, it is commonly assumed that the presence of Ly α photons strengthens the coupling of the spin to the gas temperature (See also Hirata 2006, for a more detailed calculation) and that the neutral hydrogen gas is detectable in emission around the HII regions.

In this paper, we examine whether physical conditions exist under which the WF-effect produces population inversion (i.e. $T_s < 0$) in the hyperfine levels. The possibility of population inversion via the WF-effect and the accompanying stimulated 21-cm emission has not been addressed in previous work related to EoR signals³. Varshalovich (1967) has pointed out that the WF effect could produce population inversion in the presence of strongly anisotropic Ly α emission, or when very steep cut-offs exist in the UV spectrum blueward of the Ly α line (also see Kaplan et al. 1979, for some more exotic mechanism). The first condition is difficult to meet due to the large optical depth to Ly α photons of a neutral IGM. Exploring in more detail whether $T_s < 0$ barely needs justification: if high redshift 21-cm masers exist, they could boost the 21-cm EoR signal by orders of magnitude. Interestingly, Chuzhoy & Shapiro (2006) recently showed that scattering of Ly α and Ly β photons by deuterium can cause its spin temperature to be negative. Technically, this produces a 92-cm maser, although the associated gain is too small to provide a dramatic effect.

Since the WF-effect involves scattering of Ly α photons through an optically thick medium, a proper treatment of the Ly α radiative transfer is necessary. Previous work on the WF-effect generally assumed the spatial and time derivatives in the Ly α radiative transfer equation to be zero. Without these assumptions the transfer problem becomes analytically intractable. In this paper, we demonstrate that astrophysical situations may exist, during which these assumptions are no longer valid to the extent that the Ly α

color temperature may, in fact, be temporarily negative. We investigate whether this may lead to detectable 21-cm masers.

The outline of this paper is as follows. In § 2 we calculate the gain factor associated with a negative hydrogen spin temperature. In § 3 we show how the standard definition of the Ly α color temperature can be extended to an arbitrary Ly α frequency distribution and how it affects the hydrogen spin temperature. In § 4.1 we give a simple example of a situation in which the Ly α color temperature is negative. This is followed in § 5 by a discussion on what astrophysical conditions are required to produce 21-cm masers and whether these are met by conventional sources. The total gain of 21-cm masers and whether maser saturation is an issue is discussed in § 6. Finally, in § 7 we present our conclusions. The parameters for the background cosmology used throughout this paper are $\Omega_m = 0.3$, $\Omega_\Lambda = 0.7$, $\Omega_b = 0.044$, and $h = 0.7$ (Spergel et al. 2003).

2 THE GAIN FACTOR ASSOCIATED WITH A NEGATIVE SPIN TEMPERATURE

When $T_s < 0$, stimulated emission of 21-cm emission occurs. Here, we estimate the implications for the expected gain in the total 21-cm emissivity. The change of the intensity in the line center of the 21-cm line, I , with distance, s , is given by (Rybicki & Lightman 1979),

$$\frac{dI}{ds} = -\alpha I + j, \quad (1)$$

where α is the opacity of the gas to radiation at a wavelength of $\lambda_S = 21\text{cm}$ and j is its corresponding volume emissivity. The standard solution to this equation is

$$I(s) = I(0) e^{-\alpha s} + \frac{j}{\alpha} (1 - e^{-\alpha s}). \quad (2)$$

Here, $I(0)$ is the intensity of the 21-cm photons before they enter the gas, $I(0) = 2k_B T_{\text{CMB}}/\lambda_S^2$. The 21-cm volume emissivity, j , and opacity, α , are given by

$$j = \frac{h\nu_S}{4\pi\Delta\nu_S} n_2 A_{21} \quad (3)$$

$$\alpha = \frac{h\nu_S B_{21}}{4\pi\Delta\nu_S} (3n_1 - n_2),$$

where $\nu_s = 1.4$ GHz, is the frequency of the hyperfine transition; $\Delta\nu_S = \nu_s v_{\text{th}}/c$, in which v_{th} is the thermal velocity dispersion of the atoms; A_{21} and B_{21} are the Einstein coefficients associated with the hyperfine transition. Eq. (2) can be rewritten as

$$I(s) = I(0) e^{s/R_M} - \frac{2k_B T_s}{\lambda_S^2} (e^{s/R_M} - 1), \quad (4)$$

where $R_M \equiv -1/\alpha$. We used $B_{21} = A_{21} c^2 / 2h\nu_0^3$, $n_H \sim n_1/4$ and the definition of the spin temperature (§ 1) to rewrite $j/\alpha = 2k_B T_s / \lambda_S^2$. Since for a negative spin temperature $\alpha < 0$, $I(s)$ increases exponentially with s . R_M is the length scale over which $I(s)$ increases by one factor of e and can be written as

$$R_M \equiv -\frac{1}{\alpha} \approx 0.7 \left(\frac{1+z}{11} \right)^{-3} \left(\frac{1+\delta}{20} \right)^{-1} \times \left(\frac{T_s}{-10 \text{ K}} \right) \left(\frac{T_{\text{gas}}}{10 \text{ K}} \right)^{1/2} \text{ kpc}. \quad (5)$$

³ Spaans & Norman (1997) have investigated whether hydrogen masers can exist during EoR, but they focused on hydrogen recombination lines. They found that masers may exist in the $n\alpha \sim 60$ recombination lines, where n is the principal quantum number of hydrogen and $n\alpha$ denote the transitions $n \rightarrow n-1$.

Equation (5) shows that a reasonably small region in which $T_s < 0$, also known as the ‘‘masing region’’, could produce a significant boost in $I(0)$. According to Eq. (5), the total maser amplification increases toward lower T_{gas} and $|T_s|$ values and higher densities.

3 THE $\text{Ly}\alpha$ COLOR AND HYDROGEN SPIN TEMPERATURE

3.1 The $\text{Ly}\alpha$ Color Temperature

Madau et al. (1997) defined the color temperature to be:

$$\frac{kT_\alpha}{h} = -\left[\frac{\partial \log \mathcal{N}_\nu}{\partial \nu}\right]^{-1} \approx -\left[\frac{1}{J_\alpha(\nu)} \frac{\partial J_\alpha(\nu)}{\partial \nu}\right]^{-1}, \quad (6)$$

where $\mathcal{N}_\nu = c^2 J_\alpha(\nu)/2h\nu^3$ is the photon occupation number.⁴ As is shown in Appendix A1, the more general expression for the $\text{Ly}\alpha$ color temperature that is relevant for the WF-effect, is:

$$\frac{kT_\alpha}{h} = -\frac{\int J_\alpha(\nu)\phi(\nu)d\nu}{\int \frac{\partial J_\alpha(\nu)}{\partial \nu}\phi(\nu)d\nu} = \frac{\int J_\alpha(\nu)\phi(\nu)d\nu}{\int \frac{\partial \phi(\nu)}{\partial \nu}J_\alpha(\nu)d\nu} \quad (7)$$

(which has also been derived by Meiksin, 2006, Eq. 16). Here, $\phi(\nu)$ is the normalised line profile, $\int \phi(\nu)d\nu = 1$ (e.g. Rybicki & Lightman 1979). In this paper, we will often express the frequency, ν , in terms of a dimensionless frequency variable, $x \equiv (\nu - \nu_0)/\Delta\nu_D$, where $\Delta\nu_D = \nu_0 v_{\text{th}}/c$, in which $\nu_0 = 2.46 \times 10^{15}$ Hz is the $\text{Ly}\alpha$ frequency. A negative/positive value of x corresponds to a $\text{Ly}\alpha$ photon that is redshifted/blueshifted with respect to the line center, respectively. When expressed as a function of x , $\phi(x) \sim e^{-x^2}$ in the ‘core’ and $\phi(x) \sim a/[\sqrt{\pi}x^2]$ in the ‘wing’ of the line. Here, a is the Voigt parameter, which is given by $a = A_\alpha/4\pi\Delta\nu_D = 4.7 \times 10^{-4}$ ($13 \text{ km s}^{-1}/v_{\text{th}}$), where A_α is the $\text{Ly}\alpha$ Einstein-A coefficient. The transition frequency, x_t , between core and wing is defined by $e^{-x_t^2} = a/[\sqrt{\pi}x_t^2]$. Since $\phi(\nu)$ is strongly peaked around the line center, photons in this frequency range usually dominate the contribution to the integral.

Since $\partial\phi/\partial\nu < 0$ for $\nu > \nu_0$, simplistically $T_\alpha < 0$ when there are more photons with $\nu > \nu_0$ than with $\nu < \nu_0$. However, as mentioned in § 1, repeated scattering of photons in the line core rearranges the photons in frequency such that $T_\alpha \rightarrow T_{\text{gas}}$ (Field 1959). The situation is different for photons in the far wing of the line profile, $|x| \gg 1$. Here, the probability that a photon is scattered from frequency x back into the line core in a single scattering event is extremely small (e.g. Hummer 1962). Scattering moves the photons back to the line center by an average amount of only $-1/x$ (Osterbrock 1962). Therefore, once a photon finds itself far in the line wing, it can stay there for $\sim x^2$ scattering events (Adams 1972). For a population of $\text{Ly}\alpha$ photons all of which are in the blue wing of the line: (i) $T_\alpha < 0$, and (ii) scattering does not immediately redistribute the photons in frequency space such that $T_\alpha \rightarrow T_{\text{gas}}$. Therefore, a blueshifted $\text{Ly}\alpha$ line has the potential to sustain a negative color temperature

while it interacts with the gas. This may lead to a negative spin temperature, as we discuss next.

3.2 The Hydrogen Spin Temperature

The generalised expression for the equilibrium⁵ Hydrogen spin temperature is (see Appendix A1)

$$T_s = \frac{T_{\text{cmb}} + y_\alpha T_\alpha + y_c T_{\text{gas}}}{1 + y_\alpha + y_c}, \quad (8)$$

where $y_\alpha = \frac{4P_\alpha T_* Q[J_\alpha(\nu)]}{27A_{21}T_\alpha}$ and $y_c = \frac{C_{21}T_*}{A_{21}T_{\text{gas}}}$. Here, A_{21} and B_{21} are the Einstein rate coefficients and C_{21} is the collisional de-excitation rate. This expression differs slightly from the standard expression (e.g. Madau et al. 1997)⁶. Here, $Q[J_\alpha(\nu)]$ is a function that depends on the exact $\text{Ly}\alpha$ spectral shape (see Eq. A15), and which classically obtains a value $Q[J_\alpha(\nu)] \sim 1$. However, Hirata (2006, his Eq. B.18) has recently shown that due to quantum interference term, the probability that a spin-flip occurs through scattering by $\text{Ly}\alpha$ wing photons is strongly reduced. Therefore, $Q[J_\alpha(\nu)]$ may become very small in cases in which all $\text{Ly}\alpha$ photons are in the extreme wings of the line profile. On the other hand, this quantum interference effect might be different for the situation in which a real $\text{Ly}\alpha$ photon is absorbed into a particular 2p-level of hydrogen, followed by re-emission (Zygelman, private communication). Because it is not completely obvious yet how strongly quantum interference affects the strength of the WF-coupling in the line wings, in this paper we will express our answers as a function of $Q[J_\alpha(\nu)]$, keeping in mind that it may take on very small values.

The denominator of Eq. 8 shows that $T_s < 0$ requires $P_\alpha > 27/4(T_\alpha/T_*)A_{21} \sim 3 \times 10^{-11} \text{ s}^{-1}(T_\alpha/[-100 \text{ K}])(1/Q[J_\alpha(\nu)])$, provided that the $\text{Ly}\alpha$ scattering rate dominates the collision rate and the CMB scattering rate. Since our $\text{Ly}\alpha$ photons are in the line wings, their scattering cross section is significantly reduced. To get the necessary $\text{Ly}\alpha$ scattering rate requires a large $\text{Ly}\alpha$ flux. This is most easily demonstrated by writing the $\text{Ly}\alpha$ scattering rate as

$$P_\alpha = \frac{\sigma_0}{h\nu_0} \frac{L_{\text{Ly}\alpha}}{4\pi r^2} \int \mathcal{J}(x)\phi(x)dx, \quad (9)$$

where $\mathcal{J}(x)$ is the normalised spectrum ($\int \mathcal{J}(x)dx = 1$). For a source emitting a top hat $\text{Ly}\alpha$ spectrum with $J(x) = 0$ for $x < x_{\text{min}}$ and $x > x_{\text{max}}$, the scattering rate at a distance r is

$$P_\alpha = \frac{\sigma_0}{h\nu_0} \frac{L_{\text{Ly}\alpha}}{4\pi r^2} \frac{\int_{x_{\text{min}}}^{x_{\text{max}}} \phi(x)dx}{x_{\text{max}} - x_{\text{min}}} \approx 2.6 \times 10^{-11} \text{ s}^{-1} \times \left(\frac{300 \text{ K}}{T_{\text{gas}}}\right) \left(\frac{10 \text{ kpc}}{r}\right)^2 \left(\frac{L_\alpha}{10^{44} \text{ ergs}^{-1}}\right) \left(\frac{10^5}{x_{\text{min}}x_{\text{max}}}\right), \quad (10)$$

where L_α is the total $\text{Ly}\alpha$ luminosity. For $x_{\text{min}}x_{\text{max}} = 10^5$,

⁵ This equilibrium value is reached on a timescale of $\sim P_\alpha^{-1}$, provided $\text{Ly}\alpha$ scattering is the dominant level-mixing process.

⁶ An additional (small) correction to the standard expression was recently derived by Chuzhoy & Shapiro (2006), who accounted for the change in energy of the $\text{Ly}\alpha$ photon when its absorption and re-emission results in a spin-flip. This causes $y_\alpha \rightarrow y_\alpha/(1 + 0.4T_{\text{gas}}^{-1})$ and the WF-coupling strength is somewhat reduced. Since $T_{\text{gas}} = 300 \text{ K}$ in our paper (4.3), this only changes y_α by 0.1%. This factor does not affect our results and we ignore it hereafter, especially since the quantum interference correction is substantially larger.

⁴ Note that we have omitted the $3/\nu$ -term on the right-hand-side. This is only correct when $\frac{3k|T_\alpha|}{h\nu_0} \sim (|T_\alpha|/3 \times 10^4 \text{ K}) \ll 1$.

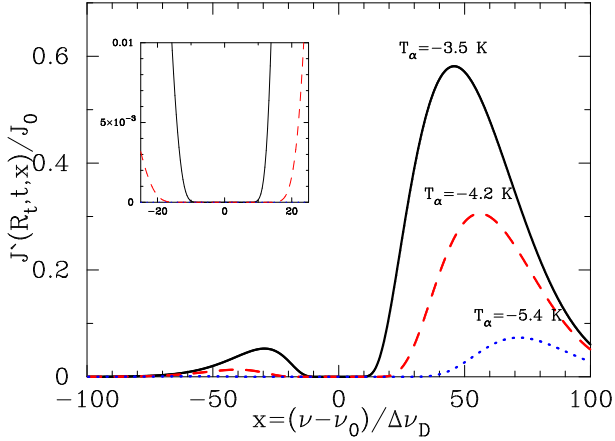


Figure 1. Three examples of Ly α spectra with a negative color temperature. These spectra were obtained after suppressing a blueshifted Gaussian emission line (with an amplitude J_0) by a factor of $e^{-\tau_0 \phi(x)}$, with $\tau_0 = 10^5$ (black solid line), $\tau_0 = 10^{5.3}$ (red dashed line) and $\tau_0 = 10^6$ (blue dotted line, see text for more details). The spectra that are shown practically contain no photons in the core of the line profile (which is shown better in the inset, which zooms on the spectra in the line core), and the majority of the photons lies blueward of the line center. The Ly α color temperature associated with each curve is shown as a label.

which is a reasonable choice (§ 4.1 and § 4.3), the total Ly α luminosity must exceed $10^{44}/Q[J_\alpha(\nu)]$ erg s $^{-1}$, which for $Q[J_\alpha] = 1$ is an order of magnitude brighter than the Ly α luminosities that are typically observed in high-redshift ($z = 6.5$) galaxies (Rhoads et al. 2004; Kashikawa et al. 2006) but fainter than that of bright quasars (Fan et al. 2006). For this top-hat spectrum, the minimum Ly α luminosity is larger by a factor of $\sim x_{\min}^2$ when the quantum inference term is incorporated (see Appendix A3).

4 $T_\alpha < 0$ IN A NEUTRAL COLLAPSING GAS CLOUD

4.1 An Illustrative Example in which $T_\alpha < 0$

The discussion in § 3.2 demonstrated that the hydrogen spin temperature can become negative in the presence of a large flux of Ly α photons that are primarily in the blue wing of the line. Here, we describe a simple model which illustrates the relevant physical conditions to make $T_\alpha < 0$ and discusses the possible duration of this phenomenon.

A Ly α point source is embedded in a neutral gas cloud that is contracting with a uniform velocity, v_i . The Ly α source is turned on at $t = 0$. The intrinsic Ly α spectrum, expressed in the dimensionless frequency variable x , is Gaussian with a standard deviation of x_c . In the frame of the infalling gas this line appears blue shifted. The spectrum at the photon front, $R_t = ct$, becomes

$$J'(R_t, t, x) = J_0 e^{-\frac{(x-x_i)^2}{2x_c^2}} \times e^{-\tau_0 \phi(x)}, \quad (11)$$

where $x_i = v_i/v_{\text{th}}$, J_0 is the amplitude of the Gaussian emission line and is arbitrary, and $\tau_0 = \sigma_0 n_H R_t$. For large values of τ_0 , the spectrum at R_t practically only contains photons in the wing of the line, the majority of which lies blueward of the line center. This is shown in Figure 1 which shows

$J'(R_t, t, x)$ for $\log[\tau_0] = 5.0$ (solid line); 5.3 (red dashed line) and 6.0 (blue dotted line), where $x_c = x_i = 30$ and the gas temperature, $T_{\text{gas}} = 10$ K. The color temperature (Eq. 7) associated with each curve is -3.5 , -4.2 and -5.5 K, respectively.

The color temperature remains negative only for a finite amount of time. The moment the core photons reach a given radius R , $T_\alpha \rightarrow T_{\text{gas}}$. The duration of time over which the color temperature remains negative determines whether the Ly α photons can establish population inversion in the hyperfine levels. It is difficult to analytically estimate by how much the core photons are delayed in their arrival at a given radius R . Resonant scattering causes a Ly α photon to undergo a random walk in frequency, which causes its mean free path to change during its random walk through space (Adams 1972; Loeb & Rybicki 1999). One consequence of this is that the average number of times a Ly α photon scatters to traverse a line center optical depth τ_0 scales as $\propto \tau_0$, as opposed to the $\propto \tau_0^2$ scaling expected for a standard random walk (Adams 1972; Harrington 1973; Neufeld 1990). The vast majority of these scattering events takes place in the line core, but spatial diffusion occurs predominantly in the line wings. The first Ly α photons that were emitted by the source in the line core to arrive at a radius R , are therefore mostly in the line wings. Similarly, frequency diffusion may cause Ly α photons that were emitted by the source in the line wing, to emerge at radius R in the line core. To properly account for these effects, the precise duration of this negative color temperature episode should be determined with a Monte-Carlo code. In the following section (§ 4.3, we give an example in which the color temperature, in fact, stays negative indefinitely).

4.2 The MC-Simulation of Ly α Radiative Transfer in a Collapsing Gas Cloud

We use the Monte-Carlo code described in Dijkstra et al. (2006) for our radiative transfer calculation. This code calculates the Ly α transfer through spherically symmetric gas clouds, with arbitrary density and velocity fields. The detailed micro-physics of Ly α scattering is incorporated in this code. For details and descriptions of tests performed on the code, the interested reader is referred to the above paper. The code was expanded for the work presented in this paper to follow the time evolution of the Ly α radiation field as a function of position. This was achieved by keeping track of the total time that elapsed since a Ly α photon was emitted. When this time reaches user-specified values, a ‘snapshot’ of the photon trajectory is taken and its location and frequency in the frame of the infalling gas is recorded.

The bright Ly α source is embedded in a neutral collapsing gas cloud. The total (dark matter + baryons) mass of the halo hosting the collapsing cloud is $M_{\text{tot}} = 10^{11} M_\odot$. Collapse occurs at redshift $z = 8$. Here, we use a more realistic gas density and velocity field compared to that of § 4.1. Within the virial radius, $r_{\text{vir}} = 16$ kpc the gas density is assumed to trace the dark matter (which is given by a NFW profile with concentration parameter $c = 5$) modified by a core at $r < 3r_s/4$ (see Maller & Bullock 2004, their Eq. 9-11) where $r_s = r_{\text{vir}}/c$. The infall velocity field, $v(r)$, is assumed to be linear with $v(r) = -v_{\text{circ}}[r/r_{\text{vir}}]$ in which $v_{\text{circ}} (= 158 \text{ km s}^{-1})$ is the circular velocity of the host

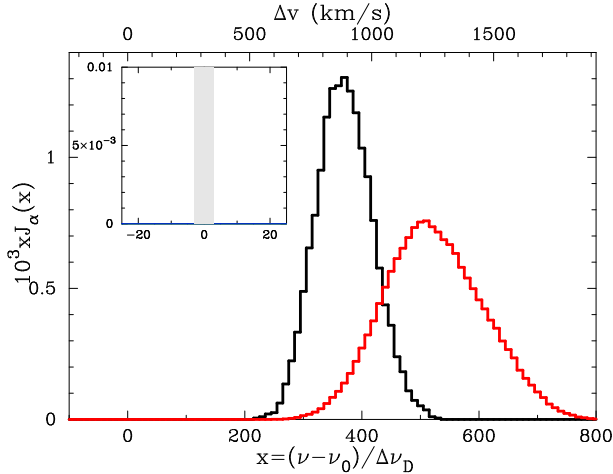


Figure 2. Time evolution of the Ly α spectrum ‘seen’ by a gas element at $r = 15$ kpc, inside a collapsing cloud of neutral hydrogen. The Ly α radiative transfer was calculated using a Monte-Carlo code. All Ly α photons are inserted at $t = 0$, and the spectra are shown at $t = 4t_{\text{cross}}$ (black) and $t = 10t_{\text{cross}}$ (red), where $t_{\text{cross}} \equiv r_{\text{sn}}/c$ is the light-crossing time to radius $r_{\text{sn}} = 15$ kpc. All spectra are systematically blueshifted relative to the line center, which is due to energy transfer from the infalling gas to the Ly α photons. These distributions of Ly α photons have $T_{\alpha} \sim -160$ K ($t = 4t_{\text{cross}}$) and $T_{\alpha} \sim -230$ K ($t = 10t_{\text{cross}}$). For $P_{\alpha} \gtrsim 5 - 7 \times 10^{-11} \text{ s}^{-1}$, $T_s < 0$.

dark matter halo. Beyond the virial radius, $r > r_{\text{vir}}$, infall of gas continues and we adopt the density and velocity profiles based on the curves shown in Figures 2 and 4 of Barkana (2004; see Dijkstra et al, 2006, for a more detailed discussion of this choice). The gas collapsing outside the galaxy is assumed to be cold, $T_{\text{gas}} = 300$ K. Recent calculations by Birnboim & Dekel (2003) have shown that virial shocks are likely not to exist in objects with masses below $M_{\text{tot}} \sim 2 \times 10^{11} M_{\odot}$ (also see Kereš et al. 2005). Our choice of T_{gas} then represents the minimum temperature that can be reached through cooling by H $_2$ molecules.

Photons are injected at $t = 0$ following a Gaussian frequency distribution with $\sigma_v = v_{\text{circ}}$. Snapshots were taken of the Ly α frequency distribution at $r_{\text{sn}} = 5, 10, 15$ and 20 kpc at four different times: $t = 4t_{\text{cross}}$, $t = 6t_{\text{cross}}$, $t = 8t_{\text{cross}}$ and $t = 10t_{\text{cross}}$, where $t_{\text{cross}} \equiv r_{\text{sn}}/c$ is the light-crossing time to radius r_{sn} . The spectra derived from these snapshots at $r = 15$ kpc are shown in Figure 2 as the black ($t = 4t_{\text{cross}}$) and red ($t = 10t_{\text{cross}}$) histogram. The Ly α photons lie systematically to the blue side of the line, by amounts greatly exceeding the infall velocity. The inset of the Figure zooms on the line core and shows more clearly that no photons are present in the core of the line profile. The reason for the large shift to the blue side of the line can be easily understood: as the Ly α photons propagate outward through an optically thick collapsing gas cloud, energy is transferred from the gas to the photons, which results in an overall blueshift of the line (Zheng & Miralda-Escudé 2002; Dijkstra et al. 2006), which can exceed the infall velocity of the infalling gas significantly (Large velocity shifts are common in Ly α radiative transfer through optically thick gas clouds. In order for Ly α to escape from an optically very thick gas cloud,

the photons need to diffuse far into the line wings, where the gas cloud becomes optically thinner).

Each subsequent timestep the Ly α line shifts slightly further to the blue and broadens. This broadening of the line can be thought of as being a direct consequence of the frequency diffusion associated with Ly α scattering. This diffusion process in a collapsing cloud has a preference of shifting the photons further to the blue.

It is interesting to note that the core photons do not emerge at all at $r = 15$ kpc (and at all radii $r > 5$ kpc). In § 4.1 we argued that core photons would eventually arrive at any radius, causing T_{α} to become positive. This argument did not take into account, however, that energy is transferred from the gas to the Ly α photons as they are propagating outward through the neutral collapsing gas cloud, causing an overall blueshift. Therefore, the color temperature of the Ly α photons emitted by the source stays negative for the entire lifetime of the Ly α source. We point out that for continuous Ly α emission, the Ly α spectrum at a given radius is some average of the spectra calculated above.

4.3 The Ly α Color Temperature and Hydrogen Spin Temperature

Using Eq (8) the Ly α color temperature associated with the four spectra of Figure 2 was calculated to be $T_{\alpha} = -160$ K at $t = 4t_{\text{cross}}$ and $T_{\alpha} = -230$ K at $t = 10t_{\text{cross}}$. Therefore, neutral collapsing gas clouds surrounding a central Ly α source, with realistic gas density and velocity profiles, see a negative Ly α color temperature.

For the color temperatures mentioned above, T_s is negative when the Ly α scattering rate $P_{\alpha} \gtrsim 5 - 7 \times 10^{-11}/Q[J_{\alpha}(\nu)] \text{ s}^{-1}$ (§ 3.2). For the spectra shown in Figure 2, Ly α luminosities exceeding a few times $10^{45}/Q[J_{\alpha}(\nu)] \text{ erg s}^{-1}$ are required to produce $P_{\alpha} \gtrsim 5 - 7 \times 10^{-11}/Q[J_{\alpha}(\nu)] \text{ s}^{-1}$ at $r = 10 - 15$ kpc (Eq. 9). To produce such high Ly α luminosities with stars requires a high star formation rate. The Ly α luminosity can be estimated as $L_{\text{Ly}\alpha} \sim 1 - 3 \times 10^{42} (\dot{M}_{*}/M_{\odot} \text{ yr}^{-1}) \text{ erg s}^{-1}$, where \dot{M}_{*} is the star formation rate (e.g. Loeb et al. 2005; Dijkstra et al. 2006b). Note that this relation assumes that stars form according to the conventional Salpeter mass function. For a top-heavy mass function of stars, the Ly α luminosity may be higher by an order of magnitude (Schaerer 2003). According to this relation, $L_{\text{Ly}\alpha} \gtrsim 10^{45}/Q[J_{\alpha}(\nu)] \text{ erg s}^{-1}$ requires $\dot{M}_{*} \gtrsim 10^3/Q[J_{\alpha}(\nu)] M_{\odot}/\text{yr}$.

Therefore, the existence of 21-cm masers depends strongly on the importance of quantum interference. When this is ignored all together, large-but physically possible-star formation rates are required to produce a maser. On the other hand, existing calculations suggest that quantum interference requires unphysical star formation rates that are a factor of $\sim 10^5$ times larger (Appendix A3). This illustrates the importance of detailed atomic physics calculations for this work.

5 CONSTRAINTS ON THE PROPERTIES OF THE CENTRAL $\text{Ly}\alpha$ SOURCE

A key requirement for a negative hydrogen spin temperature is the absence of $\text{Ly}\alpha$ photons in the line center, as these would scatter and rapidly rearrange the level populations in the hyperfine transition such that $T_s \rightarrow T_{\text{gas}}$. So far, our calculation assumed that all $\text{Ly}\alpha$ photons were emitted by the central source and that the $\text{Ly}\alpha$ core photons are delayed (indefinitely in fact in the example discussed in § 4.3) in their arrival at a given radius, as their significantly shorter mean free path reduces their spatial diffusivity. However, $\text{Ly}\alpha$ core photons may emerge at a certain location through different channels. These are discussed below in § 5.1. This is followed by a discussion in § 5.2-§ 5.3 on what is required to reduce the impact of these $\text{Ly}\alpha$ core photons, such that maser conditions prevail.

5.1 Alternative Sources of $\text{Ly}\alpha$ that can make $T_\alpha > 0$

Different channels that cause $\text{Ly}\alpha$ core photons to emerge at a certain location include:

1. $\text{Ly}\alpha$ that is produced following x-ray and Cosmic Ray heating. When hydrogen recombines after being photoionised by x-rays that managed to penetrate the neutral gas (collisional ionisation at low temperatures is negligible), a $\text{Ly}\alpha$ photon is produced with a probability of $\sim 2/3$ (for case B recombination). The emergent $\text{Ly}\alpha$ photon has a high probability of being injected close to the line center. This effect is probably not important because the recombination time $t_{\text{rec}} = 1/(n_e\alpha) \gg t_{\text{cross}}$, particularly in an almost completely neutral medium (regardless of the gas temperature). A more important effect however, is that photoionisation by x-rays may produce energetic electrons that excite the $n = 2$ level of atomic hydrogen, which immediately results in the emission of a $\text{Ly}\alpha$ core photon (e.g. Chen & Miralda-Escude 2006).

2. $\text{Ly}\alpha$ that is produced following photoexcitation by soft UV-photons. Photons in the energy range $E = 10.2 - 13.6$ eV (hereafter 'soft UV-photons') can generally easily penetrate deep into a neutral medium, where they are absorbed by neutral hydrogen atoms. Consider the example discussed in § 4.1, but assume that the central source is also emitting soft UV photons. $\text{Ly}\alpha$ photons with $|x| \gtrsim 40$ can reach the radius corresponding to $\log[\tau_0] = 5.3$, without being scattered (for these photons $\tau < 1$). However, the same applies to $\text{Ly}\gamma$ photons with $|x_\gamma| \gtrsim 5$; $\text{Ly}\delta$ photons with $|x_\delta| \gtrsim 3$, etc.⁷ To obtain these numbers, we derived the cross-sections for higher-order Lyman-series transitions in Appendix B. Whereas the $\text{Ly}\alpha$ wing photons have a negligible probability of being scattered into the line center, the higher-order Lyman-series photons have a $\sim 35\%/5 = 7\%$ probability of being converted into a $\text{Ly}\alpha$ photon that is in the line core, per scattering. The factor of 5 reflect that a higher order Lyman-series photon scatters on average ~ 5 times before undergoing a cascade (which results in a $\text{Ly}\alpha$ photon $\sim 35\%$ of the time, see Pritchard & Furlanetto 2006).

⁷ $\text{Ly}\beta$ photons can be ignored here since these have a zero probability of being transformed into $\text{Ly}\alpha$ (Pritchard & Furlanetto 2006a).

The newly produced $\text{Ly}\alpha$ -core photons interact strongly with the neutral gas. The evolution of the hydrogen spin temperature depends on which population of $\text{Ly}\alpha$ photons dominates the scattering rate that results in a spin-flip. In order for the scattering rate of the $\text{Ly}\alpha$ wing photons to dominate (and thus to make the hydrogen spin temperature negative), we show that the spectrum of the central source must be truncated strongly blueward of the $\text{Ly}\beta$ transition.

5.2 Constraints on the $\text{Ly}\alpha$ Source's Spectral Energy Distribution.

The scattering rate of the newly created $\text{Ly}\alpha$ photons following photoexcitation by soft-UV photons can be written as

$$P_{\alpha,\text{con}}(\mathbf{r}) = \frac{4}{27} \langle N \rangle \epsilon P_n(\mathbf{r}) = \quad (12)$$

$$\langle N \rangle \frac{16\pi\epsilon}{27} \int_{\text{Ly}\gamma}^{\text{Ly}\epsilon} \frac{J(\nu)}{h\nu} \sigma_{\text{tot}}(\nu) e^{-\tau(\nu,\mathbf{r})} d\nu.$$

Here, $\epsilon = 0.07$ is the mean probability for a higher-order Lyman-series (denoted by $\text{Ly}-n$) photon to be converted per scattering (Pritchard & Furlanetto 2006a), and $4/27$ is the approximate probability that a spin-flip occurs for $\text{Ly}\alpha$ photon core scattering. $P_n(\mathbf{r})$ is the scattering rate of the $\text{Ly}-n$ photons, $\tau(\nu, \mathbf{r})$ is the total optical depth of the intervening hydrogen gas between the source (at $r = 0$) and the location \mathbf{r} to photons of frequency ν . The integral is performed over $h\nu \in [12.8 - 13.6]$ eV, as $\text{Ly}\beta$ photons cannot be converted into $\text{Ly}\alpha$ photons. Furthermore, $\langle N \rangle$ is the total number of times a $\text{Ly}\alpha$ core photon scatters before it disappears.

To estimate $\langle N \rangle$, we first observe that it takes on average $\sim 10^4 - 10^5$ scattering events for a $\text{Ly}\alpha$ core photon to be scattered into the wing, $|x| > x_t \sim 3$ (Hummer 1962). However, photons close to the core-wing transition frequency, $|x_t|$, can scatter back into the line core in a single scattering event. Therefore, $\langle N \rangle$ should be higher. Velocity gradients facilitate the escape of $\text{Ly}\alpha$ photons. In the presence of velocity gradients the majority of the scattering events of a photon occurs around its resonant region. For a *static* medium, a $\text{Ly}\alpha$ photon scatters on average $\sim \tau_0$ times to traverse an optical depth τ_0 (Adams 1972; Harrington 1973). The total optical depth of the resonant region, τ_{res} , can be calculated from the total optical depth over the scale for which the velocity changes by a thermal width (also known as the Sobolev length), v_{th} : $\tau_{\text{res}} = n_H \sigma_0 v_{\text{th}} [dv_{\text{infall}}/dr]^{-1}$. If we approximate $dv_{\text{infall}}/dr \sim v_{\text{circ}}/r_{\text{vir}}$, where v_{circ} and r_{vir} are the circular velocity and virial radius of the host dark matter halo, then $\tau_{\text{res}} \sim 2 \times 10^6 [(1 + \delta)/60][(1 + z_{\text{vir}})/9]^{3/2}$. Here, δ is the overdensity of the gas. Note that the temperature dependence has cancelled out in this expression. Therefore, for a photon to escape from its local resonant region, it scatters on average $\langle N \rangle \sim \tau_{\text{res}} \sim 10^6 - 10^7$ times.

To get some sense of the magnitude of $P_{\alpha,\text{con}}$, we return to the example discussed in § 4.1. We assume that the central $\text{Ly}\alpha$ source has an additional continuum flux that is spectrally flat, i.e. $J(\nu)$ is independent of ν for $h\nu \in [10.2 - 13.6]$ eV. We will evaluate the ratio of $P_{\alpha,\text{con}}$ and P_α , the scattering rate of $\text{Ly}\alpha$ wing photons (with a negative color temperature) that results in a spin-flip, at radius r , which corresponds to $N_{\text{HI}} = 10^{17} \text{ cm}^{-2}$ (or $\log[\tau_0] = 5.3$). Here, $\tau(\nu, \mathbf{r}) = N_H \sigma_{\text{tot}}(\nu)$, where $\sigma_{\text{tot}}(\nu)$ is the absorption cross

section at frequency ν which is obtained by summing over all Lyman series transitions (derived in Appendix B). The flux density of Ly α wing photons is given by Eq. (11), and P_α is calculated using Eq. (9). The ratio of $P_{\alpha,\text{con}}$ and P_α is independent of r and is evaluated numerically and found to be

$$P_{\alpha,\text{con}}/P_\alpha \sim \langle N \rangle / (J_0 Q[J_\alpha]), \quad (13)$$

where J_0 is the amplitude of the Ly α emission line (as in Eq. (11), or more accurately, the ratio of the peak Ly α to the continuum flux density). Of course, this approximation depends on the assumed value of N_H and width of the intrinsic Ly α emission line, x_c . However, we have found the dependence on these parameters to be rather weak. According to Eq. (13), the converted Ly α photons dominate the scattering rate, unless $J_0 > \langle N \rangle / Q[J_\alpha]$, i.e. the intrinsic peak Ly α flux density must lie a factor of $\langle N \rangle \sim 10^7 / Q[J_\alpha]$ above the continuum. It is more common to express the prominence of the Ly α line through its equivalent width (EW). In this example, $\text{EW} = 0.1 J_0 \text{ \AA}$. Therefore, unless $\text{EW} > 0.1 \langle N \rangle \sim 10^6 / Q[J_\alpha] \text{ \AA}$, the Ly α scattering rate is determined by the converted Ly α photons and will drive the spin temperature to its color temperature (which is not negative). An intrinsic Ly α EW of $10^6 / Q[J_\alpha] \text{ \AA}$ is exceptionally high, several orders of magnitude above the values that are typically observed in $z = 6.5$ galaxies (Rhoads et al. 2004; Shimasaku et al. 2006).

For comparison, a normal population can theoretically produce a maximum $\text{EW} = 200\text{--}300 \text{ \AA}$. This number can be higher by about a factor of 5 for pop III stars. Therefore, it seems impossible that such large Ly α EWs exist. On the other hand, it has been shown that a multiphase interstellar medium (ISM) can transmit a significantly larger fraction of Ly α photons compared to continuum photons (Neufeld 1991; Hansen & Oh 2006) (the Ly α and UV-continuum transmission of the ISM are denoted by f_α and f_c , respectively). The exact conditions that are required in a multiphase ISM to produce the large Ly α EWs mentioned above, are discussed in § 5.3.

5.3 Requirements for the Ly α Source's ISM.

In multiphase ISM models, the ISM consists of cold, dense, dusty clumps embedded in a hot medium. The Ly α scatters off the cold clumps and propagates mainly through the hot, dust free, interclump medium. The continuum photons, on the other hand, can easily penetrate the clumps where it is subject to absorption by dust. Therefore, $f_\alpha > f_c$ and the Ly α EW is boosted.

Not surprisingly, boosting the Ly α EW by a factor of $\gtrsim 10^3$ requires extreme conditions. To minimise f_c one requires large columns of dust. The value of f_c can be estimated from $f_c = \langle e^{-\tau_d} \rangle$, where $\tau_d = N_H \epsilon_d \sigma_d$, in which N_H is the total column of hydrogen of a clump, σ_d is the dust cross section per hydrogen nuclei and ϵ_d is the probability that a continuum photon is absorbed (rather than scattered). For the diffuse HI phase of the Milky Way, $\tau_d = 0.5(N_H/10^{21} \text{ cm}^{-2})$ (Hansen & Oh 2006, and references therein), which indicates that to get $\tau_d \gtrsim 12$ (corresponding to $\langle e^{-\tau_d} \rangle \lesssim 10^{-5}$) requires $N_H \gtrsim 3 \times 10^{22} \text{ cm}^{-2}$, provided these clumps have the same dust content. To maximise f_α one requires to minimise the number of these clumps (or

to maximise their sizes). We point out that local starburst galaxies may have gas surface density well in excess of this value (see e.g. Fig 2 of Thompson et al. 2006), with columns reaching values $\gtrsim 10^{24} \text{ cm}^{-2}$. Of course, high redshift galaxies are expected to be less massive, but if we approximate the gas surface density as $\Sigma_{\text{gas}} \propto M_{\text{gas}}/R_{\text{gas}}^2 \propto M_{\text{halo}}/R_{\text{vir}}^2 \propto M_{\text{halo}}^{1/3} (1 + z_{\text{vir}})^2$, then we find that systems with masses lower by a factor of 10^3 that virialised at $z \gtrsim 6$ (vs. $z \sim 1$ for local starburst galaxies), may possess comparable or bigger gas surface densities. Therefore, the crucial factor that determines whether Ly α EW $\gtrsim 10^6 / Q[J_\alpha] \text{ \AA}$ can theoretically exist, is the distribution of the gas inside these galaxies. We have verified that the large column of dust and gas mentioned above would also suppress the x-ray flux enough for Ly α production via x-ray heating to be negligible.

6 THE GAIN OF THE MASER

We return to the collapsing gas cloud described in § 4.3. We consider the scenario in which the WF-effect makes the hydrogen spin temperature negative, and estimate the the gain of the maser. The exponential increase in intensity of radiation passing through the masing region (Eq 4) only continues as long as Ly α pumping can maintain the population inversion against the growing losses by stimulated emission. The expression for the equilibrium hydrogen spin-temperature in the presence of an amplified 21-cm radiation field modifies to

$$T_s = \frac{\mathcal{G}T_{\text{cmb}} + y_\alpha T_\alpha + y_c T_{\text{gas}}}{1 + y_\alpha + y_c}. \quad (14)$$

Here, \mathcal{G} is the maser amplification of the background radiation field. When $\mathcal{G} \rightarrow \infty$, $T_s \rightarrow \infty$ and the intensity only increases linearly with path-length. According to Eq A9, saturation starts to become important when $\mathcal{G}T_{\text{cmb}} = y_\alpha T_\alpha = \frac{4P_\alpha T_s}{27 A_{21} Q[J_\alpha(\nu)]}$, which for $P_\alpha T_s / Q[J_\alpha(\nu)] = 5 - 7 \times 10^{-11} \text{ s}^{-1}$ (§ 4.3) yields $\mathcal{G} \sim 250$. Therefore, maser saturation does not become important until the total maser amplification reaches a value of ~ 250 .

The Ly α transfer code provides us with Ly α spectra at $r = 5, 10, 15$ and 20 kpc . We calculate T_α at each radius, ignoring for simplicity the slight variation in T_α with time, and use Eq. (8) to calculate T_s at these radii. We assume that the WF-coupling is strong enough to cause $T_s \sim T_\alpha$. The length scale that is relevant to calculate the total gain is given by the Sobolev length, ℓ_S , which is the length over which the velocity changes by less than the thermal velocity, $\ell_S = v_{\text{th}} / [dv(r)/dr]$. For the example calculated above, $\ell_S = v_{\text{th}} R_{\text{vir}} / v_{\text{circ}} = 0.014 (T_{\text{gas}}/300\text{K})^{1/2} R_{\text{vir}}$. The total gain γ is then estimated from the product $\ell_S \times \alpha$, in which α is given by Eq. (3). We find that $\gamma = 3 \times 10^{-3} (|T_s|/200\text{K})^{-1} (1 + \delta)/40$, which is independent of the gas temperature. Since the total maser amplification is given by $\mathcal{G} \equiv e^\gamma \sim 1.003$, this does not provide a dramatic effect.

To get a larger gain of the maser we need a larger Sobolev length ℓ_S . The Sobolev length can be increased for a different infall velocity field $v(r)$. In particular, for decelerating inflows with $dv/dr < 0$ one may construct velocity fields that give an arbitrarily long Sobolev length

(Rybicki & Hummer 1978).⁸ Although this requires some fine tuning, the gain factor can be considerably larger than the value quoted above.

The gain is potentially larger when coherent clumps of gas, such as mini-halos (defined as objects with a virial temperature below the hydrogen cooling threshold $T_{\text{vir}} < 10^4$ K), are present in the infalling gas. Furlanetto et al. (2006) give the line-center optical depth τ to 21-cm radiation through the center of the mini-halo, $\tau \sim 0.026[(1+z)/10]^{1/2}(M_{\text{tot}}/10^7 M_{\odot})^{-2/3}$. This τ is related to our gain factor, γ , via $\gamma = \tau \bar{T}_{\text{gas}}/|T_s|$, in which $\bar{T}_{\text{gas}} \sim T_{\text{vir}}$ is the mean temperature of the virialised gas in the mini-halo. For $T_s = -200$ K, we obtain⁹ $\gamma = 0.5[(1+z)/10]^{1/2}$ (which is independent of mass). The factor e^{γ} increases dramatically for denser mini-halos that collapsed at higher redshift (as long as collisional excitation of the 21-cm line inside these denser mini-halos does not bring T_s towards T_{gas}), and for lower values of $|T_s|$. However, from the previous calculations it seems unlikely that γ can be increased by an additional factor $\gtrsim 10$ and $\gamma_{\text{max}} \sim 5$. Note that for $\gamma \sim 4.6$ the 21cm flux from the CMB is amplified by a factor of $e^{\gamma} \sim 100$ (see Eq. 4). This maximum magnification would cause the brightness temperature of these minihalos to be enhanced to $T_b \sim 100(\lambda_S^2/2k) I_{\text{CMB}} \sim 100 \times T_{\text{CMB},0} = 270$ K, but in a narrow frequency range of $10(T_{\text{gas}}/300 \text{ K})^{1/2}$ kHz, and on an angle on the sky of ~ 0.1 arcsec, where the exact number depends on the minihalo mass and redshift (note that both the frequency range and the angular extent of 21-cm maser emission is enhanced when more minihalos were present in the collapsing gas).

7 CONCLUSIONS

We have explored the prospects for a population inversion in the hyperfine levels of atomic hydrogen at high redshifts when the Universe was still predominantly neutral. The existence of 21-cm masers during the epoch of reionisation (EoR) could greatly boost the expected EoR signals.

We have performed Monte-Carlo calculations of the radiative transfer of Ly α photons emitted by a source embedded in a neutral collapsing gas cloud and computed the Ly α spectrum as function of radius and time. After deriving an expression for the Ly α color temperature T_{α} for arbitrary frequency distributions of Ly α photons (Eq. 7), this expression was used to show that neutral collapsing gas clouds

⁸ For example, a velocity field of the form $v(r) = -r/\sqrt{r^2 - l^2}$, for $r > l$, gives an infinitely large Sobolev length at impact parameter l .

⁹ The Ly α radiative transfer is affected by the presence of dense minihalos in the infalling gas. In order to investigate whether the Ly α color temperature remains negative inside the minihalo gas, a 3-D Monte-Carlo calculation of the Ly α transfer should be performed. Here, we only point out that the total column of hydrogen through mini-halos is typically $N_H = 10^{20} - 10^{21} \text{ cm}^{-2}$. Ly α photons blueshifted by more than $v \gtrsim (a\tau)^{1/3} v_{\text{th}} = 200 - 400(T_{\text{gas}}/10^4 \text{ K})^{1/6} \text{ km s}^{-1}$, can propagate through these clouds without being scattered in the line core, as required for the Ly α color temperature to remain negative inside the mini-halo. Since the spectra shown in Figure 2 satisfy this requirement, it seems possible for the population of Ly α photons shown in Figure 2 to cause population inversion in the mini-halo gas.

surrounding a central Ly α source, with realistic gas density and velocity profiles, see a negative Ly α color temperature.

We have investigated whether a population inversion in the hyperfine transition via the Wouthuysen-Field effect can be established in such scenarios, thus resulting in a 21-cm maser. Classically, Ly α luminosities exceeding $\sim 10^{44} - 10^{45} \text{ erg s}^{-1}$ (which can be obtained with physically possible star formation rates of $\dot{M}_{*} \gtrsim 10^3 M_{\odot} \text{ yr}^{-1}$) are required to produce a population inversion. However, the astrophysical conditions that are required to establish such a population inversion are very difficult to meet for two reasons:

- Quantum interference can strongly reduce the strength of the WF-effect in the Ly α line wings: As was shown by Hirata (2006), the probability that a spin-flip occurs when a Ly α wing photon scatters is reduced by a factor of $Q[J_{\alpha}] \sim (x_{45}/x)^2$ (see Appendix A3) when quantum interference is included. In the context of this paper, this factor can be as small as $Q[J_{\alpha}] \sim 10^{-4} - 10^{-6}$ and increases the required Ly α luminosities by a factor of $1/Q[J_{\alpha}]$. The exact degree at which quantum interference reduces the spin-flip probability far in the line wings may be affected by a possible deviation from a Lorentzian line profile far in the line wings (Zygelman, 2007, in preparation).

- A key requirement for having $T_{\alpha} < 0$ is the absence of Ly α photons in the line center, as these would scatter and rapidly rearrange the level populations in the hyperfine transition such that $T_s \rightarrow T_{\text{gas}}$. We discussed in § 5 that Ly α core photons can be injected at a given location via two different channels: (1) Photoionisation by x-rays that penetrate the neutral gas can produce energetic electrons which can excite the $n = 2$ level of atomic hydrogen, which immediately results in the emission of a Ly α core photon. (2) Soft-UV photons ($E \in [10.2 - 13.6] \text{ eV}$) can generally easily penetrate deep into a neutral medium, where they can photoexcite neutral hydrogen atoms. These atoms have a probability of ~ 0.07 of re-emitting a Ly α core photon. The negative impact of these newly produced Ly α photons (both by x-rays and soft-UV photons) can theoretically be overcome under extreme conditions in the ISM in which a Ly α line emerges from the galaxy with a Ly α EW $\gtrsim 10^6/Q[J_{\alpha}] \text{ \AA}$.

For completeness, we have calculated the total associated maser gain associated with the gas clouds that may see a negative Ly α color temperature. In order to obtain a substantial path length, one requires minihalos to be embedded inside the gas that is collapsing onto the Ly α emitter. This could produce a maximum amplification of the background CMB photon-field that is $\mathcal{G} \lesssim 100$. We find saturation not to be an issue. We conclude that it appears very unlikely for maser activity to be detected by forthcoming low frequency observatories. Conversely, if anomalously high 21-cm fluxes are found, this could be indicative of extraordinary astrophysical conditions in and around the first galaxies.

Acknowledgments We thank George Rybicki and Stuart Wyithe for useful discussions. MD would like to thank Harvard's Institute for Theory & Computation for its hospitality. MD is supported by the Australian Research Council. AL was supported in part by NASA grants NAG 5-1329 and NNG05GH54G.

REFERENCES

- Adams, T. F. 1972, *ApJ*, 174, 439
- Birnboim, Y., & Dekel, A. 2003, *MNRAS*, 345, 349
- Chen, X., & Miralda-Escudé, J. 2004, *ApJ*, 602, 1
- Chen, X., & Miralda-Escudé, J. 2006, submitted to *ApJ*, astro-ph/0605439
- Chuzhoy, L., & Shapiro, P. R. 2006, *ApJ*, 651, 1
- Dijkstra, M., Haiman, Z., & Spaans, M. 2006, *ApJ*, 649, 14
- Dijkstra, M., Lidz, A., Wyithe, J.S.B. 2006b, Submitted to *MNRAS*
- Fan, X., et al. 2006, *AJ*, 132, 117
- Field, G. B. 1959, *ApJ*, 129, 551
- Furlanetto, S. R., & Loeb, A. 2002, *ApJ*, 579, 1
- Furlanetto, S. R., & Loeb, A. 2004, *ApJ*, 611, 642
- Furlanetto, S. R. 2006, *MNRAS*, 371, 867
- Furlanetto, S. R., Oh, S. P., & Briggs, F. H. 2006, *Physical Review*, 433, 181
- Hansen, M., & Oh, S. P. 2006, *MNRAS*, 367, 979
- Harrington, J. P. 1973, *MNRAS*, 162, 43
- Hirata, C. M. 2006, *MNRAS*, 367, 259
- Hummer, D. G. 1962, *MNRAS*, 125, 21
- Iliev, I. T., Shapiro, P. R., Ferrara, A., & Martel, H. 2002, *ApJL*, 572, L123
- Kaplan, S. A., Kleinman, E. B., & Oiringel, I. M. 1979, *Soviet Astronomy Letters*, 5, 184
- Kashikawa, N., et al. 2006, *ApJ*, 648, 7
- Kereš, D., Katz, N., Weinberg, D. H., & Davé, R. 2005, *MNRAS*, 363, 2
- Loeb, A., & Rybicki, G. B. 1999, *ApJ*, 524, 527
- Loeb, A., & Zaldarriaga, M. 2004, *Physical Review Letters*, 92, 211301
- Loeb, A., Barkana, R., & Hernquist, L. 2005, *ApJ*, 620, 553
- Madau, P., Meiksin, A., & Rees, M. J. 1997, *ApJ*, 475, 429
- Maller, A. H., & Bullock, J. S. 2004, *MNRAS*, 355, 694
- Meiksin, A. 2000, in *Perspectives on Radio Astronomy*, Published by ASTRON. ISBN: 90-805434-1-1, 340 pages, 2000, p.37, 37–+
- Meiksin, A. 2006, *MNRAS*, 370, 2025
- Menzel, D. H., & Pekeris, C. L. 1935, *MNRAS*, 96, 77
- Neufeld, D. A. 1990, *ApJ*, 350, 216
- Neufeld, D. A. 1991, *ApJL*, 370, L85
- Osterbrock, D. E. 1962, *ApJ*, 135, 195
- Peebles, P. J. E. 1993, *Princeton Series in Physics*, Princeton, NJ: Princeton University Press, —c1993,
- Peterson, J. B., Pen, U., & Wu, X. 2006, *Astronomical Society of the Pacific Conference Series*, 345, 441
- Pritchard, J. R., & Furlanetto, S. R. 2006a, *MNRAS*, 367, 1057
- Pritchard, J. R., & Furlanetto, S. R. 2006b, submitted to *MNRAS*, astro-ph/0607234
- Rhoads, J. E., et al. 2004, *ApJ*, 611, 59
- Rybicki, G. B., & Hummer, D. G. 1978, *ApJ*, 219, 654
- Rybicki, G. B., & Lightman, A. P. 1979, *Radiative processes in astrophysics* (New York, Wiley-Interscience, 1979. 393 p.)
- Schaerer, D. 2003, *A&A*, 397, 527
- Scott, D., & Rees, M. J. 1990, *MNRAS*, 247, 510
- Shimasaku, K., et al. 2006, *PASJ*, 58, 313
- Spaans, M., & Norman, C. A. 1997, *ApJ*, 488, 27
- Spaans, M., & Silk, J. 2006, submitted to *ApJ*, astro-ph/0601714
- Spergel, D. N., et al. 2003, *ApJS*, 148, 175
- Thompson, T. A., et al. 2006, *ApJ*, 645, 186
- Venkatesan, A., Giroux, M. L., & Shull, J. M. 2001, *ApJ*, 563, 1
- Varshalovich, D. A. 1967, *Soviet Physics JETP*, 25, 157
- Wouthuysen, S. A. 1952, *AJ*, 57, 31
- Zheng, Z., & Miralda-Escudé, J. 2002, *ApJ*, 578, 33
- Zygelman, B. 2006, in preparation

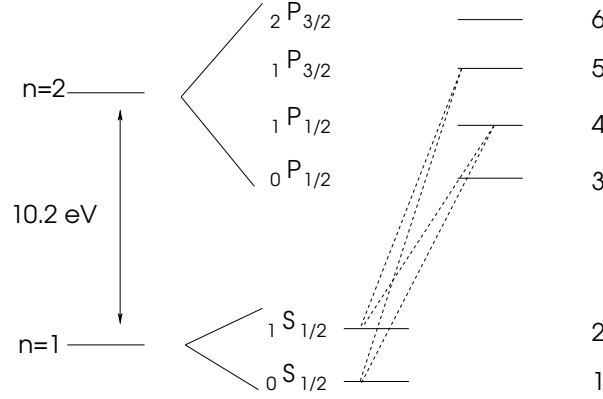


Figure A1. Schematic depiction of hyperfine splitting of the electronic ground state ($n=1$) and the first excited state ($n=2$) of the hydrogen atom. This 6-level model has been used to arrive at the expressions for the Ly α color temperature, Eq. A7 and the spin temperature, Eq. A9. The *dashed lines* denote the transitions involved in the mixing of hyperfine levels. Levels 3 and 6 do not contribute to the mixing of levels. The notation used for the individual levels is FLJ , where L is the orbital angular momentum, J the total angular momentum quantum number. Here, F is the sum of J and I , the nuclear spin quantum number.

APPENDIX A: DERIVATION OF THE LY α COLOR AND HYDROGEN SPIN TEMPERATURE

A1 The 6-Level Hydrogen Atom without Collisions and CMB photons

In this section we derive the expression for the Ly α color temperature taking into account hyperfine splitting in the Hydrogen atom's $n = 1$ and $n = 2$ states, following Meiksin (2000). Ignoring collisions and absorption and re-emission of CMB photons, the rate equation for atoms in the $n = 1$ state is

$$\begin{aligned} \frac{\partial n_1}{\partial t} &= n_2 A_{21} + \bar{J} \left[-B_{14} \frac{A_{42}}{A_{42} + A_{41}} n_1 + B_{24} \frac{A_{41}}{A_{41} + A_{42}} n_2 - B_{15} \frac{A_{52}}{A_{52} + A_{51}} n_1 + B_{25} \frac{A_{51}}{A_{51} + A_{52}} n_2 \right] = \\ &= n_2 A_{21} + \bar{J} \frac{c^2}{2h\nu_0^3} \left[-\frac{g_4}{g_1} \frac{A_{41} A_{42}}{A_{42} + A_{41}} n_1 + \frac{g_4}{g_2} \frac{A_{42} A_{41}}{A_{41} + A_{42}} n_2 - \frac{g_5}{g_1} \frac{A_{51} A_{52}}{A_{52} + A_{51}} n_1 + \frac{g_5}{g_2} \frac{A_{52} A_{51}}{A_{51} + A_{52}} n_2 \right] \end{aligned} \quad (\text{A1})$$

where we used the relations $B_{du} = \frac{g_u}{g_d} B_{ud} = \frac{g_u}{g_d} \frac{c^2}{2h\nu_0^3} A_{ud}$, and the notation $\bar{J} \equiv \int J(\nu) \phi(\nu) d\nu$. Following Meiksin (2000),

$$A_{41} = \frac{1}{3} A_\alpha, \quad A_{42} = \frac{2}{3} A_\alpha, \quad A_{51} = \frac{2}{3} A_\alpha, \quad A_{52} = \frac{1}{3} A_\alpha, \quad , \quad (\text{A2})$$

where $A_\alpha = 6.25 \times 10^8 \text{ s}^{-1}$, is the total Einstein A-coefficient, and $g_1 = 1$, $g_2 = 3$, $g_4 = 3$ and $g_5 = 3$. We get

$$\frac{\partial n_1}{\partial t} = n_2 A_{21} + \frac{c^2}{2h\nu_0^3} A_\alpha \left[-\frac{2}{3} n_1 \int J(\nu) \phi_{14}(\nu) d\nu + \frac{2}{9} n_2 \int J(\nu) \phi_{24}(\nu) d\nu - \frac{2}{3} n_1 \int J(\nu) \phi_{15}(\nu) d\nu + \frac{2}{9} n_2 \int J(\nu) \phi_{25}(\nu) d\nu \right]. \quad (\text{A3})$$

All line profiles are the same, apart from an offset in frequency: $\phi_{24}(\nu) = \phi_{14}(\nu + \Delta\nu_S)$, $\phi_{25}(\nu) = \phi_{15}(\nu + \Delta\nu_S)$ and $\phi_{14}(\nu) = \phi_{15}(\nu + \Delta\nu_G)$, where $\Delta\nu_G = 10.89 \text{ Ghz}$ and $\Delta\nu_S = 1.42 \text{ Ghz}$ (Hirata 2006). If we approximate $\phi(\nu + \Delta\nu) \approx \phi(\nu) + \Delta\nu \frac{\partial \phi}{\partial \nu}$ and write everything in terms of ϕ_{15} (which is written as $\phi(\nu)$ hereafter), and replace n_2 with $n_H - n_1$, we get

$$\frac{\partial n_1}{\partial t} = n_2 A_{21} + \frac{c^2}{9h\nu_0^3} A_\alpha \left[n_H \int J(\nu) \left(2\phi(\nu) + \frac{\partial \phi}{\partial \nu} \Delta\nu_G + 2 \frac{\partial \phi}{\partial \nu} \Delta\nu_S \right) d\nu - n_1 \int J(\nu) \left(8\phi(\nu) + 4 \frac{\partial \phi}{\partial \nu} \Delta\nu_G + 2 \frac{\partial \phi}{\partial \nu} \Delta\nu_S \right) d\nu \right]. \quad (\text{A4})$$

This can be written in the following more compact form

$$\frac{\partial y}{\partial t} = (1 - y) A_{21} + b_1 - b_2 - y(4b_1 - b_2) \quad (\text{A5})$$

after dividing the left and right hand side of Eq A4 by n_H and after writing $y = n_1/n_H$ and where we defined

$$b_1 \equiv A_\alpha \frac{c^2}{9h\nu_0^3} \int J(\nu) \left(2\phi(\nu) + \frac{\partial \phi}{\partial \nu} \Delta\nu_G \right) d\nu; \quad b_2 \equiv -A_\alpha \frac{2c^2}{9h\nu_0^3} \Delta\nu_S \int \frac{\partial \phi}{\partial \nu} J(\nu) d\nu \quad (\text{A6})$$

The equilibrium value of y is obtained by setting $\partial y/\partial t=0$ and corresponds to a spin temperature T_s of

$$T_s \approx \frac{3y}{4y-1} T_* = -\frac{b_1}{b_2} T_* = \left[\frac{\int \phi(\nu) J(\nu) d\nu}{\Delta\nu_S \int \frac{\partial \phi}{\partial \nu} J(\nu) d\nu} + \frac{\Delta\nu_G}{\Delta\nu_S} \right] T_* \approx \left[\frac{\int \phi(\nu) J(\nu) d\nu}{\Delta\nu_S \int \frac{\partial \phi}{\partial \nu} J(\nu) d\nu} \right] \equiv T_\alpha, \quad (\text{A7})$$

where we have used that the second term within the square brackets is negligible compared to the first term for all applications in this paper. Here the last definition only states that if Ly α scattering were the dominant process regulating the level populations in the 21 cm transition, then the equilibrium spin temperature is equal to the Ly α color temperature. Since $h\Delta\nu_S = k_B T_*$, this yields Eq. (7).

A2 The 6-Level Hydrogen Atom with Collisions and CMB photons

In the presence of CMB photons and when collision are accounted for, Eq. (A5) changes to

$$\frac{\partial y}{\partial t} = (1 - y)(A_{21} + C_{21} + B_{21}I_{\text{CMB}}) + (b_1 - b_2) - y(4b_1 - b_2 + C_{12} + B_{12}I_{\text{CMB}}). \quad (\text{A8})$$

In this case the equilibrium solution (obtained by setting $\partial y/\partial t=0$) corresponds to a spin temperature T_s of

$$T_s \approx \frac{3y}{4y-1}T_* = \frac{T_* + \frac{C_{21}}{A_{21}}T_* + \frac{B_{21}}{A_{21}}I_{\text{CMB}}T_* + \frac{b_1-b_2}{A_{21}}T_*}{1 - \frac{b_2}{A_{21}} + \frac{C_{21}T_*}{A_{21}T_{\text{gas}}}} = \frac{T_* + \frac{C_{21}}{A_{21}}T_* + \frac{B_{21}}{A_{21}}I_{\text{CMB}}T_* + \frac{b_1(1+\frac{T_*}{T_\alpha})T_*}{A_{21}}}{1 + \frac{b_1T_*}{A_{21}T_\alpha} + \frac{C_{21}T_*}{A_{21}T_{\text{gas}}}}, \quad (\text{A9})$$

where we used that $B_{12} = 3B_{21}$ and $C_{12} = 3C_{21}e^{-T_*/T_{\text{gas}}} \approx 3C_{21}(1 - T_*/T_{\text{gas}})$. When the Ly α scattering rate is expressed as

$$P_\alpha = 4\pi \int \frac{J(\nu)}{h\nu} \sigma(\nu) d\nu \approx \frac{4\pi}{h\nu_0} \frac{B_\alpha h\nu_0}{4\pi} \int J(\nu) \phi(\nu) d\nu = 3A_\alpha \frac{c^2}{2h\nu_0^3} \int J(\nu) \phi(\nu) d\nu \sim \frac{27}{4}b_1, \quad (\text{A10})$$

the standard equation for the hydrogen spin temperature (e.g. Madau et al. 1997) is recovered:

$$T_s = \frac{T_* + T_{\text{cmb}} + y_\alpha T_\alpha + y_c T_{\text{gas}}}{1 + y_\alpha + y_c}, \quad y_\alpha = \frac{4P_\alpha T_*}{27A_{21}T_\alpha}, \quad y_c = \frac{C_{21}T_*}{A_{21}T_{\text{gas}}}, \quad (\text{A11})$$

where T_* in the numerator is usually omitted as it is negligibly small compared to the other terms in most applications.

A3 Expressions of T_α and T_s with Quantum Interference

Hirata (2006) has performed detailed quantum mechanical calculations of the cross-section of the process in which absorption and re-emission of Ly α photons results in a transition between levels 1 and 2 (Fig A1). These cross-sections are denoted as σ_{12} and σ_{21} and represent the transitions $1 \rightarrow 2$ and $2 \rightarrow 1$, respectively. They are given by

$$\sigma_{12} = \frac{2}{9}\sigma_0[\phi_{14} + \phi_{15} - 2\phi_{15/14}], \quad \sigma_{21} = \frac{2}{27}\sigma_0[\phi_{24} + \phi_{25} - 2\phi_{25/24}]. \quad (\text{A12})$$

Here, σ_0 is the Ly α cross-section evaluated at resonance and $\phi_{15/14}$ and $\phi_{25/24}$ are quantum interference terms¹⁰ which are defined as

$$\phi_{15/14}(\nu) = \frac{1}{\sqrt{2\pi}\sigma_\nu} \int d\nu' e^{-(\nu-\nu')^2/2\sigma_\nu^2} \phi_{15/14}^u(\nu'); \quad \phi_{15/14}^u(\nu) = \frac{\gamma}{\pi} \frac{\Delta\nu_{14}\Delta\nu_{15} + \gamma^2}{[\Delta\nu_{14}^2 + \gamma^2][\Delta\nu_{15}^2 + \gamma^2]}, \quad (\text{A13})$$

(and $\phi_{25/24}$ is defined equivalently) where $\sigma_\nu = \sqrt{\frac{k_B T_{\text{gas}}}{m_p c^2}} \nu_0$, in which $m_p = 1.66 \times 10^{-24}$ g is the proton mass. Furthermore, $\gamma \equiv A_\alpha/4\pi$, $\Delta\nu_{15} = (\nu - \nu_{15})$, where ν_{15} is the frequency at resonance of the $1 \rightarrow 5$ transition (Hirata 2006, the other symbols are defined similarly). For comparison, a normal 'unconvolved line profile' is given by a Lorentzian $\phi_{15}^u(\nu) = \frac{\gamma}{\pi} \frac{1}{\Delta\nu_{15}^2 + \gamma^2}$ (e.g. Rybicki & Lightman 1979, Eq 10.73). For Ly α scattering in the line core, the quantum interference term is typically smaller than the traditional terms and it can be ignored without introducing a large error. However, in the far line wings this holds not true: combining Eq A12 and Eq A13 the line profiles $\phi_{12}(x)$ and $\phi_{21}(x)$ far in the line wing can be written as

$$\phi_{12} = \frac{4}{9} \frac{a}{\sqrt{\pi}x^2} \left(\frac{x_{45}}{x}\right)^2, \quad \phi_{21} = \frac{4}{27} \frac{a}{\sqrt{\pi}x^2} \left(\frac{x_{45}}{x}\right)^2, \quad \text{with quantum interference}, \quad (\text{A14})$$

where $x_{45} = (\nu_{14} - \nu_{15})/\Delta\nu_D$. For comparison

$$\phi_{12} = \frac{4}{9} \frac{a}{\sqrt{\pi}x^2}, \quad \phi_{21} = \frac{4}{27} \frac{a}{\sqrt{\pi}x^2}, \quad \text{without quantum interference.}$$

Therefore, the probability that a spin-flip occurs when a Ly α wing photon scatters is reduced by a factor of $(x_{45}/x)^2$ when quantum interference is included. In this paper, this factor can be as small as $10^{-4} - 10^{-6}$! We caution that the exact degree at which quantum interference reduces the spin-flip probability is uncertain. The main reason for this uncertainty is that the unconvolved line profiles may deviate from Lorentzian in the far line wings, which affects these calculations (Zygelman, private communication).

Regardless of whether quantum interference is included, we can write $\phi_{21}(\nu) \equiv \sigma_{21}(\nu)/\sigma_0 = \frac{1}{3}\phi_{12}(\nu + \Delta\nu_S)$. If we then

¹⁰ Note that when the quantum interference terms are ignored the rate equation for n_1 can be written as $\frac{\partial n_1}{\partial t} = n_2(A_{21} + P_{21}) - n_1 P_{12}$, where $P_{12/21}$ is the rate at which Ly α scattering puts atoms from the $1 \rightarrow 2/2 \rightarrow 1$ state. This can be written as $\frac{\partial n_1}{\partial t} = n_2(A_{21} + 4\pi n_2 \int \frac{J(\nu)}{h\nu} \sigma_{21}(\nu) d\nu - 4\pi n_1 \int \frac{J(\nu)}{h\nu} \sigma_{21}(\nu) d\nu)$. If we use Eq A12 and ignore the quantum interference term, we are left with Eq A3. Therefore, apart from the quantum interference term, our calculations are in exact agreement with those presented by Hirata (2006).

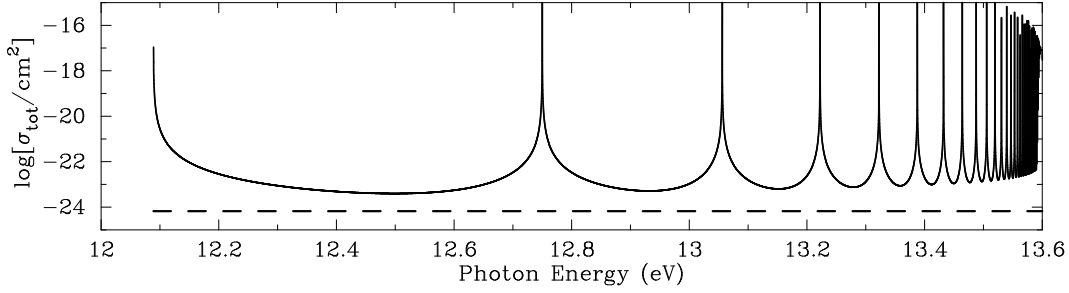


Figure B1. The absorption cross section of neutral atomic hydrogen gas to soft UV photons. The spikes at $E=12.1, 12.8, 13.05, \dots$ correspond to the $\text{Ly}\beta, \text{Ly}\gamma, \text{Ly}\delta, \dots$ -resonances, respectively. The horizontal dashed line corresponds to the Thomson cross-section.

repeate the analysis of §A1, it can be shown that the expression for the $\text{Ly}\alpha$ color remains the same. However, in the expression for the hydrogen spin temperature $y_\alpha \rightarrow y_\alpha Q[J_\alpha(\nu)]$ where

$$Q[J_\alpha(\nu)] = \frac{\int J_\alpha(\nu)[\phi_{24} + \phi_{25} - 2\phi_{25/24}]d\nu}{\int J_\alpha(\nu)[\phi_{24} + \phi_{25}]d\nu}. \quad (\text{A15})$$

This equation simply states that the in the calculation of the spin-flip rate, the cross-section that includes quantum interference should replace the cross-section that ignores this term. Note that if all $\text{Ly}\alpha$ were far in the line wings, then $Q[J_\alpha] \propto x^{-2}$.

APPENDIX B: THE OPACITY OF GAS TO PHOTONS IN THE ENERGY RANGE $E = 10.2 - 13.6$ EV.

The cross section for $\text{Ly}\alpha$ absorption can be written as

$$\sigma_\alpha(x) = \sigma_{\alpha,0}\phi(x; A_{21}) = f_{12} \frac{\pi e^2}{mc} \frac{1}{\sqrt{\pi}\Delta\nu_0} \phi(x; A_{21}), \quad (\text{B1})$$

where $\sigma_{\alpha,0}$ is the line center cross section, $f_{12} = 0.4167$ the $\text{Ly}\alpha$ oscillator strength and $\phi(x; A_{21})$ is the Voigt function (Rybicki & Lightman 1979, p. 288, Eq. 10.70). The reason for writing the voigt function as $\phi(x; A_{21})$ is that it explicitly demonstrates that it depends on the Einstein A-coefficient (in the wing of the line profile, $\phi(x) = a/[\sqrt{\pi}x^2]$, where $a = A_{21}/4\pi\Delta\nu_D$). Similarly, the cross section for higher order Lyman-series photons can be expressed as:

$$\sigma_n(x_n) = f_{1n} \frac{\pi e^2}{mc} \frac{1}{\sqrt{\pi}\Delta\nu_n} \phi(x_n; A_{n1}). \quad (\text{B2})$$

Here, $x_n = (\nu - \nu_n)/\Delta\nu_n$. To compute the cross sections therefore requires knowledge of the the oscillator strengths, f_{1n} , and the Einstein coefficients, A_{n1} . Menzel & Pekeris (1935) derived the oscillators strengths (Eq. 10.46 in Rybicki & Lightman 1979) to be

$$f_{1n} = \frac{2^9 n^5 (n-1)^{2n-4}}{3(n+1)^{2n+4}}. \quad (\text{B3})$$

From the definition of the oscillator strength we know that

$$\frac{\pi e^2}{mc} f_{1n} = \frac{h\nu_n}{4\pi} B_{1n} = \frac{g_n}{g_1} \frac{h\nu_n}{4\pi} B_{n1} = \frac{g_n}{g_1} \frac{h\nu_n}{4\pi} A_{n1} \frac{c^2}{2h\nu_0^3} \quad (\text{B4})$$

(Rybicki & Lightman 1979, Eq. 10.70). A combination of Eqs. (B3) and (B4) yields A_{1n} .

Given the cross-sections for the various Lyman-series transitions, it is possible to calculate the opacity of neutral gas for a photon of any given energy in the range $E = 10.2 - 13.6$ eV, by summing over all Lyman-series transitions

$$\sigma_\nu = \sum_{i=1}^{\infty} \sigma_i(x_i), \quad x_i = (\nu - \nu_i)/\Delta\nu_i. \quad (\text{B5})$$

The result of this calculation is shown in Figure B1.